Material characterization of advanced cement-based encapsulation systems for efficient power electronics with increased power density

B. Boettge[1], F. Naumann[1], S. Behrendt[2], M. G. Scheibel[3], S. Kaessner[4,5], S. Klengel[1], M. Petzold[1], K. G. Nickel[5], G. Hejtmann[4], A.-Z. Miric[3], R. Eisele[2]
[1]Fraunhofer Institute for Microstructure of Materials and Systems IMWS, 06120 Halle, Germany
[2]FuE-Zentrum Fachhochschule Kiel GmbH, 24149 Kiel, Germany
[3]Heraeus Deutschland GmbH & Co. KG, 63450 Hanau, Germany
[4]Robert Bosch GmbH, 71272 Renningen, Germany
[5]University of Tuebingen, Geosciences, Applied Mineralogy, 72074 Tuebingen, Germany
bianca.boettge@imws.fraunhofer.de

***Abstract*—The paper introduces novel phosphate cement- and calcium aluminate cement-based material systems with enhanced thermal, mechanical and thermomechanical properties for the encapsulation of power electronic devices and modules. These materials are aiming at improving the high-temperature operation potential of power electronic systems and thus, to promote a successful application of wide bandgap power devices in power electronics. The main focus of the study consists in a thorough material characterization of the novel cement-based encapsulants including high resolution microstructural analysis combined with a modelling approach to support material design optimization. A second task consists in the analysis of interactions of the encapsulants with the electronic material interfaces, e.g. the top-side metallization of power semiconductors, substrate metallizations and bonding wires. Furthermore, power cycling tests coupled with a comprehensive failure analysis have been carried out comparing IGBT power modules with standard silicone gel encapsulation and cement-based encapsulation. The results highlight the potential of the novel cement-based encapsulants on reliability improvements at high-temperature operation.**

Keywords- Automotive and power electronics packaging; high-temperature electronics; failure analysis techniques and materials characterization; materials for harsh environments; cement-based encapsulation

I. INTRODUCTION

Miniaturization and a corresponding increase in power density are major trends in power electronics targeting at optimum efficiency of power electronic systems during industrial application. In addition, the current development trend in automotive electronics industry characterized by an increasing market introduction of hybrid and electric vehicles is pushing the requirements for power electronic components regarding high-temperature robustness, system integration capabilities, reliability and cost efficiency [1]. In this context, wide band gap (WBG) power semiconductors, such as silicon carbide (SiC) and gallium nitride (GaN), play an important role as they have the capability to process electric power at higher voltages and temperatures with smaller die areas and less power losses [2, 3]. These characteristics do not only result in superior power conversion efficiency but enable significantly reduced volumes also at system level, due to decreased cooling requirements and smaller passive components, also contributing to overall lower costs. However, reduced device sizes and higher switching frequencies are accompanied by an increased power loss density of WBG-semiconductors resulting in increased operation temperatures of up to more than 200 °C. Thus, several material and design innovations in WBG power module packaging are under development to realize the required robustness and reliability properties, and to promote a successful industrial application of WBG power semiconductors [4]. In particular, currently applied encapsulation materials such as epoxy compounds and silicon gels can only be used for maximum operation temperatures of up to about 175 °C but will deteriorate at higher temperatures of more than 200 °C due to thermal degradation effects. Consequently, a further increase in power electronics efficiency and reliability at high-temperature operation can only be achieved by novel encapsulation materials with higher temperature stability, improved heat conductance and adapted thermomechanical properties [5]. As a consequence, also inorganic materials such as calcium aluminate cements (CAC) and phosphate cements (PC) promising an intrinsically high thermal stability are currently under evaluation. This material class seems to represent an attractive option provided that the reliability-affecting properties such as thermal conductivity, thermomechanical stability, insulation capability or chemical inertness can be accordingly adapted to the requirements of power electronic components.

The cement materials introduced in this paper are intended to withstand operation temperatures of up to 300 °C and to achieve a thermal conductivity of 5 to 10 W / (m*K) (compared to prior requirements of < 2 W / (m*K)) while minimizing thermomechanical stresses on the power semiconductor devices due to adapted coefficients of thermal expansion. The main focus of the presently running research activities consists in a thorough material characterization of the new encapsulants including high resolution microstructural analysis and the characterization of the thermomechanical behavior based on mechanical testing and micromechanical material modeling. A second task consists in the analysis of interface reactions of the cement-based systems with common electronic materials, e.g. the

2377-5726/18/$31.00 ©2018 IEEE
DOI 10.1109/ECTC.2018.00194

aluminum (Al) top-side metallization of power semiconductor devices, the copper (Cu) metallization of direct copper bonded (DCB) substrates, and Al bonding wires. Within this paper, specific focus is given to present the analysis and modelling methodology and to discuss the currently derived experimental results with respect to the developments planned in future. Furthermore, first power cycling tests combined with comprehensive failure analysis have been carried out on IGBT power modules comparing both standard silicone gel and cement-based encapsulation. These preliminary results indicate a superior reliability potential of the new encapsulation approach.

II. NOVEL CEMENT-BASED ENCAPSULATION SYSTEMS

Most polymeric materials, such as epoxies and silicones exhibit limited thermal stability based on their respective bond dissociation energies. To overcome these limitations, thermodynamically more robust electrically insulating materials, such as ceramics and minerals can be considered for application. However, processing of such materials typically requires high sintering temperatures far beyond the thermal limitations of semiconductor and electronic packaging materials. One of the technically applied exceptions is given by hydraulic binder systems, better known as cements. These materials have also a ceramic–like microstructure but can be formed at ambient temperature. Cements are formed from readily soluble starting materials (cement clinker) that harden under water uptake due to lower solubility of the formed water-containing phase. This water-containing phase forms needle-like crystals in the cement clinker grains that grow together forming a water-resistant hardened material after complete solidification [6]. Most cement systems, such as Portland cement, result in high pH-values. As a consequence, cements may form a chemically reactive medium resulting in a high risk of unwanted interface reaction for metal contact materials, such as the aluminum of the semiconductor conducting system. Consequently, compatibility to the electronic components to be encapsulated is one of the major challenges during the development of cement-based systems for power electronics.

A. Phosphate cement (PC) based encapsulants

Phosphate-bonded cement, well known for example in dental applications, is formed by the reaction between an acid, such as phosphoric acid or hydrogen phosphate salts with a base, commonly a metal oxide. The reaction results in the formation of insoluble hydrated salts upon water uptake as reaction products [7]. The choice of the metal oxide strongly depends on its reactivity and defines the application and processing properties, such as the rheology and reaction time of the respective cement paste. Commonly used metal oxides are zinc oxide and magnesium oxide. The final cement phases require high solubility products, such as Newberite ($MgHPO_4$ x $3H_2O$) as the main phase in magnesia phosphate cements [8]. In addition, chemically robust fillers are added to the cement to create a composite and to allow a fine-tuning of the material properties, such as coefficient of thermal expansion (CTE), thermal conductivity and material density. Further adjustment of the cement paste properties is performed by special additives, such as setting retarders and superplasticizers. Furthermore, specialized adhesion promoters are added to control the interaction of the hardened material with functional surfaces of the electronic components, such as chip and substrate metallizations.

B. Calcium aluminate cement (CAC) based encapsulants

A second -more technically common- cement type to be considered is based on calcium aluminate cement (CAC). CAC is characterized by its fast setting properties and chemical and thermal resistance [9]. CAC in combination with alumina is mainly applied for refractories and is also part of according research work [10-12]. The specifically developed CAC-based encapsulation material investigated in this study represents a novel type of µm-scaled composite, containing small amounts of CAC and fine-grained alumina filler, thus forming a CAC-ceramic composite (CCC). First detailed investigations on the thermal behavior and microstructure evolution of CCC are subject of a recently submitted publication [13]. The CCC material is processed at temperatures of about 60 °C, forming stable hydrate phases via cement hydration reactions [14]. Comparable to PC-based systems, the CAC material sets at higher pH-values and needs to be adapted with respect to potential corrosion effects with metallization and packaging contacts. A comparatively high thermal conductivity of above 5 W / (mK) provides high temperature application potential also for passive electronic components, such as for miniaturized transformers and coils. Furthermore, gap filling capabilities of up to 10 µm and perfect flowability represent advantages in comparison to other encapsulants, such as silicones or epoxies. Similar to PC-based cement encapsulants, the material properties and the rheological behavior can be fine-tuned by the type of fillers and suitable additives.

III. MATERIALS AND METHODS

A. Test specimen and test conditions

Within the paper, three types of test specimen were used for the different research objectives. The following chapters describe the used types of samples and the related main investigation topics.

1) Bulk material samples: Figure 1 shows the sample geometry type with a CCC-specimen on the left and a PC-specimen on the right. These samples were used to study the microstructure of the cement-based materials by cross-section analysis using high resolution scanning electron microscopy (SEM) and by computer tomography (CT) X-ray inspection. As the image contrast and the quality of the CT X-ray analysis depends on the differences in absorption coefficients and the absorption length during X-ray propagation the sample size had to be accordingly adapted to provide optimum analysis conditions [15]. On that account bulk samples of both materials were produced by sawing with samples size of about 3 mm x 3 mm x 1.5 mm.

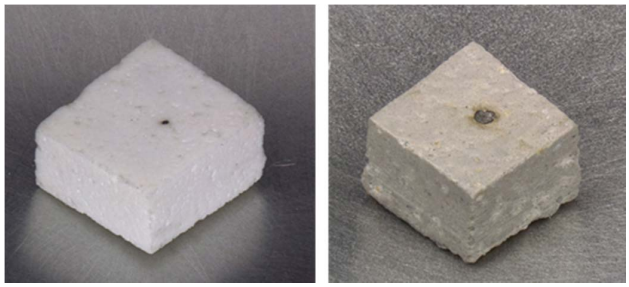

Figure 1. Material samples of CCC (left) and PC (right) based encapsulation systems.

2) Test vehicles: Special test vehicles were assembled to investigate the potential chemical and electrochemical interactions of the cement-based encapsulants with the electronic components, particularly the contact interfaces of power modules. The test vehicles consist of a diode or an IGBT soldered or sintered to a direct copper bonded (DCB) substrate. Subsequent to the die-attach process, the top-side of the power semiconductor was contacted by aluminum wire bonding and then encapsulated by different cement-based material systems. Figure 2 shows exemplarily a half-encapsulated test vehicle with a soldered power diode on a DCB substrate and Al bonding wire top-side contact.

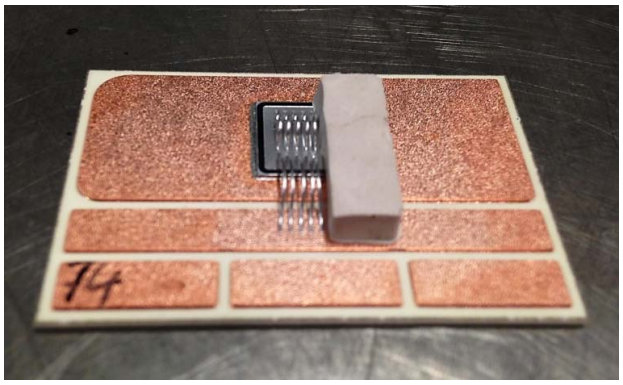

Figure 2. Half-encapsulated test vehicle, showing the silicon diode soldered to a DCB substrate and connected by aluminum wire bonding.

To study the possible interface reactions under different loading conditions, the test vehicles were investigated directly after the encapsulation process and additionally after reliability testing including High Temperature Reverse Bias (HTRB) and High Humidity High Temperature Reverse Bias (H^3TRB) testing.

The HTRB test is conventionally used to evaluate the top side isolation properties of the semiconductor. Its main objective consists in studying potential effects due to ionic impurities within these structures. The acceleration in testing by both high temperature and the electrical field is due to a higher mobility rate of the ions while the electric potential provides an increased driving force for ionic migration. These high stress effects could even result in the destruction of the device [16]. The tests were performed at the maximum blocking voltage of the IGBT at 600 V [17] and at a temperature of 150 °C.

The H^3TRB test is designed to determine any deterioration effects on the isolation of non-hermetic devices under the constant influence of humidity. Degradation effects are triggered by moisture vapor penetrating through the isolating materials. Common failure mechanisms that occur under this harsh environment are surface corrosion as well as ionic migration that were also in focus of the present investigation. During the tests, the samples were stored inside a climate chamber to apply the required relative humidity of 85 % at a temperature of 85 °C while a maximum blocking voltage of 80 V was used [18]. Failures were defined by detecting an increase in leakage current of more than 100 % compared to its initial value [19].

3) Mini power modules (MiniPIM): To investigate the thermomechanical behavior of cement-based encapsulants close to real application conditions, and to provide a more detailed understanding of relevant failure risks, mini power modules (MiniPIM) were produced and stressed by power cycling tests. The mini modules are typical frame modules of the "MiniPIM"-series produced by Danfoss Silicon Power consisting of two DBC substrates, soldered onto a standard copper baseplate. Each substrate contains two IGBTs and two diodes which are attached by a solder joint and contacted on the top-side by Al-wire bonding. Figure 3 shows exemplarily a MiniPIM power module with complete phosphate cement-based encapsulation.

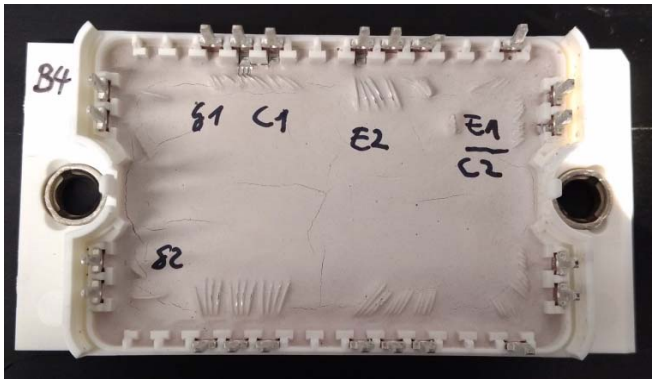

Figure 3. Mini power module (MiniPIM) for power cycling tests.

Prior to encapsulation, one of the semiconductors per substrate was electrically separated, so only one of the two IGBTs was stressed during the power cycling test. Thus, the electrically isolated IGBT remains as reference in close vicinity to the tested device.

The power cycling test simulates the real use condition of power electronic devices and evaluates the reliability of the composed electronic system. During testing the devices are turned on and off repeatedly under defined conditions,

until the end of life (EOL) of the devices [17]. A common failure mechanism of standard power modules with silicone gel encapsulation consists in wire bond lift-offs. This failure mode is caused by the thermomechanical-induced displacements within the soft-gel encapsulants. In the context of this study this test was performed to analyze the impact of cement based encapsulants, on the thermomechanical reliability properties of the investigated power modules. On that account, six power modules with standard silicone gel encapsulation were test in comparison to three power modules with PC cement-based encapsulation. Short power cycles (PC_{sec}) were performed, using the parameters given in TABLE I. on a TLW23 test bench (Schuster Elektronik GmbH, Herzogenaurach, Germany).

TABLE I. PARAMETERS OF POWER CYCLING TEST

t_{on} [s]	t_{off} [s]	I_{pulse} [A]	$T_{j,min}$ [°C]	$T_{j,max}$ [°C]	ΔT [K]	T_m [°C]
1	8	100	20	150	130	85

B. Material characterization

For material characterization, non-destructive and destructive material characterization methods were applied as described in the following section. Prior to analysis, part of these methods had first to be adapted to the complex material characteristics of the novel cement-based encapsulants.

1) Analysis of the microstructure: The microstructural characteristics of the cement-based material systems, such as filler size and filler distribution, pores, voids or cracks, have a high impact on the resulting thermal, mechanical and thermomechanical properties. On that account, 2D and computer tomography (CT) X-ray inspection using a nanomex system (General Electric Sensing & Inspection GmbH previously Phoenix, Wunstorf, Germany) was applied to investigate the microstructure of material samples. For quantitative data evaluation, the program VGStudio MAX 3.0 (VolumeGraphics GmbH, Heidelberg, Germany) was used. Furthermore, X-ray inspection was used to provide information on the quality of test vehicles and miniPIM modules. Beside non-destructive analysis, cross sections of all three specimen groups were prepared to get detailed information on the cement matrix microstructure for the material samples and on the interface reactions and particular failure modes after specific electrical testing for the test vehicles and miniPIM modules. Samples were embedded in fluorescent epoxy resin (Struers, Willich, Germany) and prepared by stepwise metallographic grinding and polishing steps. The produced cross sections of the material samples were additionally argon ion-milled using a JEOL cross section polisher (JEOL GmbH, Freising, Germany) to obtain maximum surface quality allowing to differentiate between the phases of the cement-matrix and the different filler particles. The optical inspection of the cross sections was carried out using a light optical microscope Leica DMRXE and the digital microscope DVM6A (Leica Microsystems, Heerbrugg, Switzerland). For high resolution analysis of specific interfaces scanning electron microscopy (SEM) using a Zeiss Supra-55 VP (Carl Zeiss Microscopy GmbH, Oberkochen, Germany) was applied.

2) Microstructural simulation for material design: In addition to experimental analysis also modelling of the microstructure effects on the functional material properties was performed. This simulation approach was implemented in the study to provide a more rapid screening of the influence of different filler particles and other structural features, such as pores or voids, on the resulting thermal, mechanical and thermomechanical characteristics as a function of cement composition and processing. Thus, the approach aims at supporting and accelerating the material development and microstructure design optimization by reducing the time of development and the experimental efforts. For this purpose, a Finite Element based homogenization tool Digimat-FE [20] was used to generate representative volume elements (RVE) of specific cement-based encapsulants with defined filler contents. Based on these models a screening of the influence of different filler particles, filler sizes and distributions on the CTE, the thermal conductivity and on Young's modulus of the resulting encapsulation materials was carried out.

However, for modeling the specific cement-based encapsulants also several material input-parameters are needed. Geometric size, form and distribution data of the encapsulants' microstructure were derived from high resolution optical and SEM microstructural analysis. Material properties of the containing fillers and of the matrix material, including different cement-phases, have been either taken from supplier's information or have been determined by detailed material characterization efforts within this investigation. In particular, the required temperature- dependent mechanical filler properties were derived from nanoindentation experiments using an Agilent Nano Indenter G200 with an XP transducer, and a heating stage option. Further data include CTE, young's modulus and thermal conductivity measured at different hydration states of the cement with details to be published elsewhere. The applied combination of mechanical testing and theoretical modelling by finite element (FE) simulations will, in addition to supporting the material design and system development, also form an advantageous base to future investigations of the reliability and lifetime characteristics of power electronic modules with cement-based encapsulation.

IV. Results and Discussion

A. Microstructure of cement based encapsulants and material design

In this chapter, the methodology in combining experimental microstructural analysis and microstructure design modelling will be presented for the example of a CCC-based material system. To understand, and furthermore even to predict the correlation between microstructure and material properties, such as CTE, young's modulus and thermal conductivity, detailed information on the composition of the cement matrix, on used filler particles, and the related particle size distribution, as well as on the present voids and its size distribution is required. These data have partially been taken from supplier information [13] but have been in addition, experimentally determined by reflected light microscopy and SEM cross section analysis as well as by 3D X-ray computer tomography.

1) Microstructural parameters: To demonstrate the methodology, Figure 4 gives an example of the image processing procedure to derive an according quantification of the microstructural properties from 2D cross sections for a specific cement formulation. On the left of Figure 4 the original SEM image of a cross section analysis is shown. The image in the middle represents the resulting binarized objects of the SEM image, and the image on the right of Figure 4 represents the identification of the filler size distribution and aspect ratios by statistical evaluation.

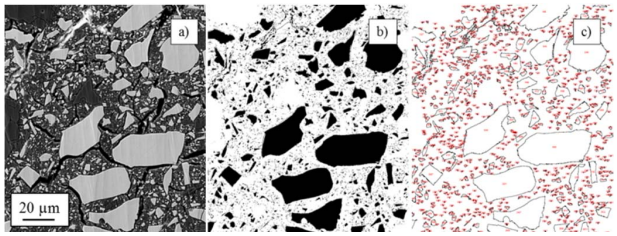

Figure 4. Estimation of the filler size distributions by 2D-microstructural analysis: a) SEM image of the cross section, b) binarization of the SEM image by digital image processing, c) statistical evaluation of filler sizes

In addition, CT X-ray analysis was used to quantitatively assess properties related to porosity and voids but also to the distribution of larger particle sizes. Figure 5 shows exemplarily the result of a CT X-ray analysis and the related data evaluation. Image processing tools have been applied to separate a specific part of the filler size distribution for better quantification of the microstructure.

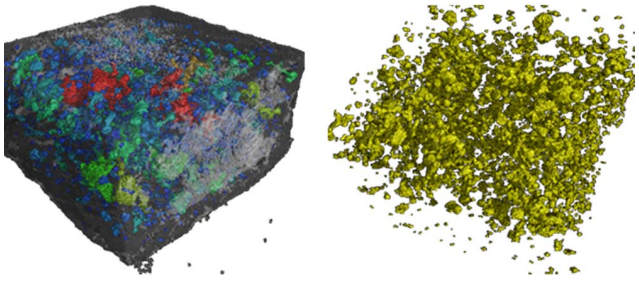

Figure 5. CT X-ray analysis: a) 3D representation of the filler size distribution, b) Separation of one filler size group

For the material under consideration, the experimental data suggested a superposition of three different filler size distributions I-III, as shown in Figure 6. Each of the single distributions could be approximated by different normal- and uniform distribution density functions. The image on the right of Figure 6 shows a generated representative volume element (RVE) of the defined filler content with different collars for each filler distribution function (I-III).

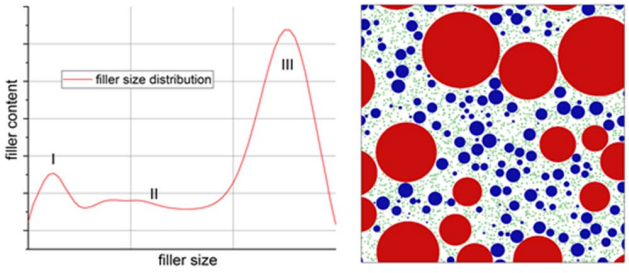

Figure 6. Size distribution of the filler particles (left) and the resulting RVE (right) of a CAC-based material system.

2) Microstructural simulation for material design: The general approach of microstructural simulation of cement-based encapsulants is illustrated in Figure 7 for a RVE representing the particular case of a filler content of 50 % and a porosity of 10 %. Using the Finite Element based homogenization tool Digimat-FE [19], a global loading is applied to the specific RVE, and the calculated response can be used to estimate the resulting material properties. In the particular case of Figure 7 a mechanical displacement was applied to the RVE allowing to determine the homogenized reaction force of the element. As a result, information on material stiffness and, thus on Young's modulus of the material can be theoretically derived.

In the next steps, also both a thermal loading by either homogenous temperature increase or temperature gradients were applied. This procedure allows predicting further homogenized material properties like CTE or thermal conductivity can be predicted in close similarity to Young's modulus.

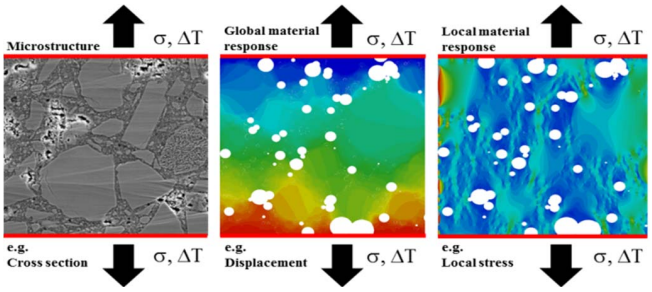

Figure 7. Simulation approach for a CCC-based material system: left: microstructure, middle: application of a global load to the RVE, right: resulting load reaction.

First results of a systematic study of the influence of specific filler contents to the resulting physical properties of a CAC-based encapsulant without porosity are exemplarily shown in Figure 8. Assuming the defined filler size composition and a spherical shape of the particles a maximum package density is reached at approximately 73 % defining the upper limit for simulation. The graph shows the influence of the analyzed Al_2O_3 filler content to the resulting Young's modulus (blue lines), the thermal expansion coefficient CTE (red lines) and the thermal heat conductivity (black lines). An increasing filler content causes a distinct reduction of the CTE on the one hand, and an increase of the thermal conductivity and Young's modulus on the other hand. Small fluctuations of the graphs are based on the specific generated geometry of the RVE by the algorithm. The graph illustrates the linking of the corresponding physical properties using a specific filler composition. This means, if one desired specification of one physical property is defined, also the other properties can be determined. Further adjustments of the material properties require the addition of other components to the cement composition. The accuracy of the obtained numerical results is limited by the available material input data and further effects – such as the influence of material interfaces (e.g. thermal transfer resistance) – which are quite complex. Nevertheless, the proposed study allows a quick screening of the potential properties of a defined filler composition and supports the material development.

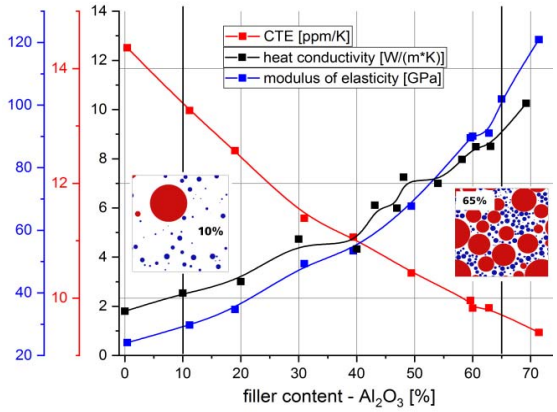

Figure 8. Systematic study of the influence of a specific filler content to the resulting physical properties of the packaging material without porosity.

Figure 9 shows the calculated influence of the porosity on the material properties for a constant Al_2O_3 filler content of approximately 50 %. As expected, significant reduction of both the heat conductivity and elastic modulus with increased porosity can be found. In this case, higher fluctuations of the graph can be observed caused by the limitations of gaining high filler content with increased porosity. This is due to the fact that a higher number of voids influences also the filler packing ratio with both factors affecting the resulting material properties.

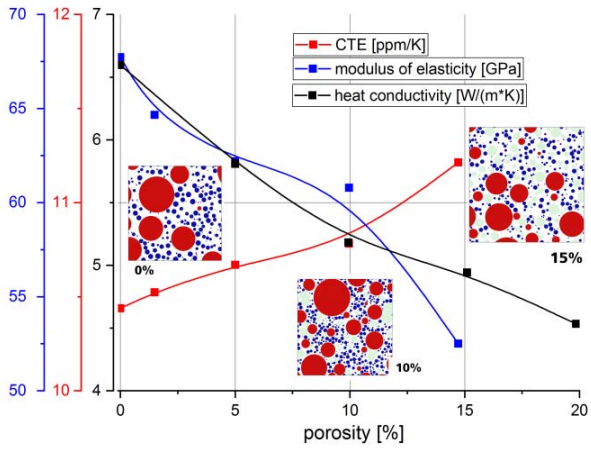

Figure 9. Calculation of the influence of porosity to material properties.

In addition to global reactions, also the local effects on the stress fields can be studied to get further insight into the interactions between voids and particles and the matrix. This is of particular high interest for a brittle material like cement where crack formation and strength properties are essentially affected by local stress concentrations formed at defects and material interfaces. This is exemplarily demonstrated in Figure 10 showing the calculated maximum stress distribution in the cement under an external mechanical displacement (a) or after temperature variation (b) where local stress is caused by CTE-mismatch between matrix and filler. In both cases local stress concentrations caused by the differences in the elastic material properties and increasing cracking risks were indicated. Thus, the material modelling approach presented here will also be useful for getting detailed insight e.g. in the strength properties of the cement materials which will be important to avoid brittle cracking during future reliability studies. Furthermore, it provides important input parameters and variables for future finite element (FEA) simulations in order to predict the reliability and lifetime characteristics of cement-based encapsulation systems.

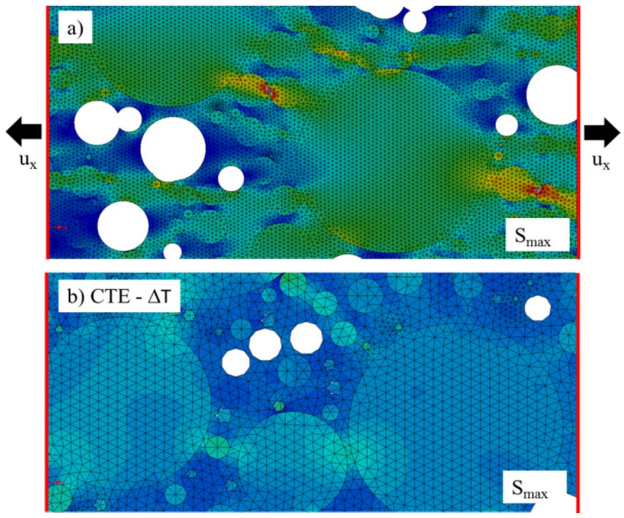

Figure 10. Calculated stress distribution (S_{max}): a) under external displacement and b) under thermal heating.

B. *Interactions at material interfaces*

The aim of the second part of the study was to investigate potential chemical and electrochemical interactions of the novel encapsulants with electronic components of power modules at critical contact interfaces, such as Al bonding wire, Cu DCB metallization and Al pad surface of the IGBT. According test vehicles were encapsulated by the cement-based material systems and subsequently stressed by HTRB or H^3TRB test as described in section III. The relevant interfaces between the cement-based encapsulant and metal interfaces were studied by microstructural analysis of samples prepared in cross section. As a general result, it was found that the H^3TRB test showed the highest impact on material degradation, compared to untested vehicles or test vehicles after HTRB test. The specifically harsh environmental conditions, including high humidity in combination with high temperatures, are initiating and accelerating ionic migration and electrochemical reactions at the analyzed interfaces. This is exemplarily demonstrated in the following figures representing typical SEM cross section analysis results for a test vehicle with PC-based encapsulation. Figure 11 presents the interface microstructure of the cement matrix with an Al bonding wire. The image on top indicates an area with direct contact between wire and cement-based encapsulant (red rectangle) and regions with gaps (blue rectangle) due to insufficient filling of the encapsulant. A close up at higher magnification reveals that the surface of the bonding wire that was not in direct contact with the cement-based encapsulant appears as very smooth and intact (Figure 11 b)). The image below (Figure 11c)), showing the bonding wire in direct contact with the cement-matrix, indicates that the wire's Al surface is chemically modified by the cement-based encapsulant. In addition, formation of a thin interface layer between the Al wire and the cement-based encapsulant is obvious, presumably due to a reaction of the aluminum with the basic cement-matrix. Further studies are necessary to clarify whether this observation results indicate a continuously progressing surface reaction or whether the interface layer can also act as a passivation layer preventing further degradation of the Al bonding wire.

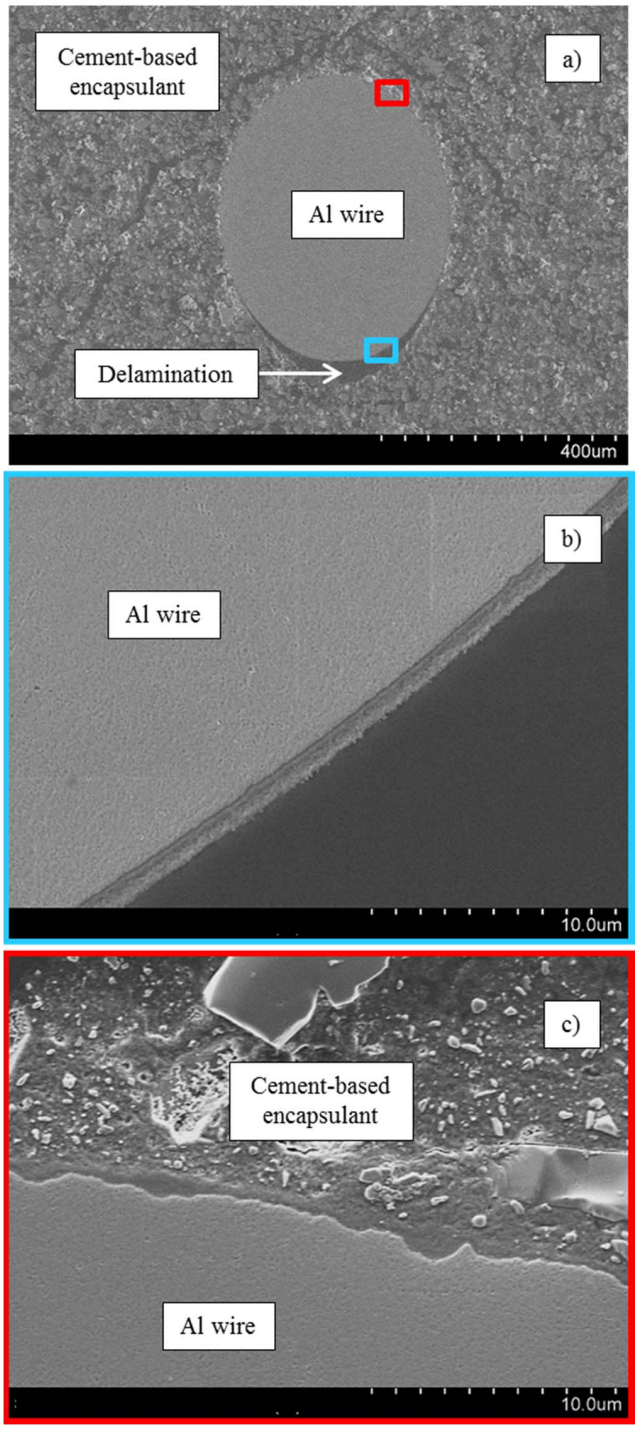

Figure 11. a) SEM image of the contact interface between Al bonding wire and cement-based encapsulation system. Detail b) No direct contact to the cement-based encapsulant (gap): intact Al-wire with an insulating varnish layer. Detail c) Direct contact to the cement-based encapsulant: Al bonding wire shows a rough surface and a thin interface layer.

Figure 12 shows the Al top-side metallization of the power IGBT in contact with the cement-based encapsulant. Comparable to the Al bonding wire, the Al top-side metallization is again converted by the cement-matrix. Remarkably, there is a significant difference in surface modification intensity when the reaction with bonding wires and the chip metallization is compared.

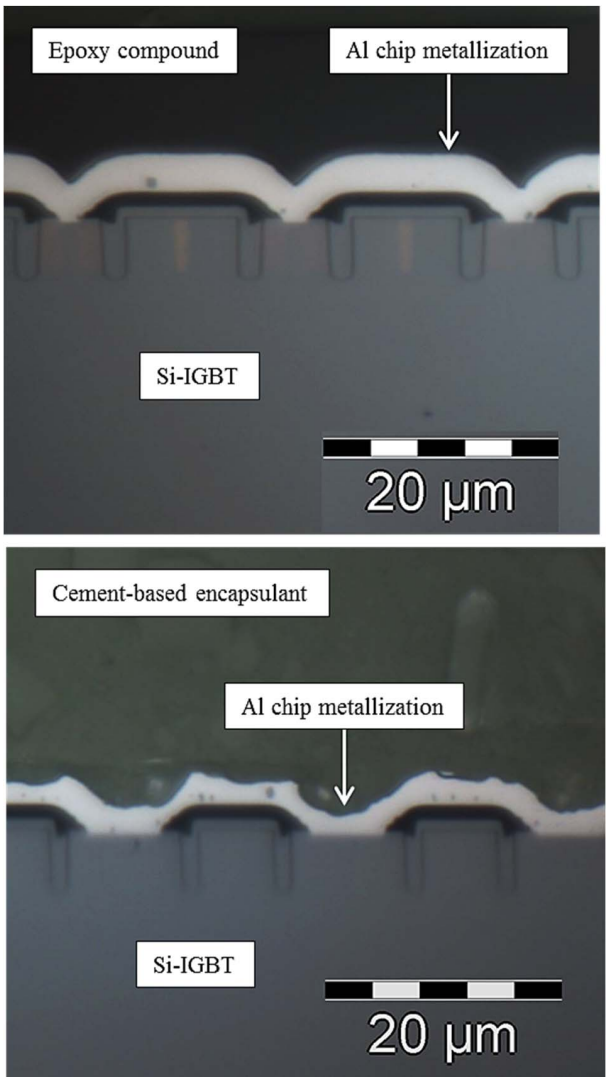

Figure 12. Light microscopic image of the contact interface between the Al metallization of the IGBT top-side and a) an epoxxy compound and b) the cement-based encapsulant.

Factors initiating the higher reaction rate at the semiconductor metallization include the different chemical composition (Al wire vs. AlSiCu chip metallization), and variation in the local testing conditions during the H^3TRB test with applied electrical voltage, leading to electrical field effects and increased ion mobility due to an increased temperature for the chip metallization. In particular, it was shown in [21, 22] that the electrochemical activity of Al is commonly lower as compared to an AlSiCu alloy. Furthermore, static electric fields that are highest at the chip surface can accelerate reactions by directing anionic contaminations along coulomb fields towards positively charged surfaces. This effect was also shown to support Al oxidation and dissolution [23]. In general, the reaction of the power semiconductor device metallization with the cement based encapsulant seems to be less critical, as device fails caused by this new failure type is much slower than conventional failure modes, such as bond wire lift offs (see power cycling results below). However, the optimization of the material compatibility of the cement-based materials with aluminum surfaces remains as one of the main topics within future work.

In contrast to aluminum, the copper surface of the DCB substrate indicates no reaction with the cement-based encapsulants, as shown in Figure 13. This might be attributed to the well-known higher redox potential of Cu (E1/2 = +0.34 V) as compared to Al (E1/2 = -1.66 V) [24]. The higher resistivity of copper metallization against reaction with cement-like materials might also be interesting in case power semiconductors with Cu metallization will be used in future [25].

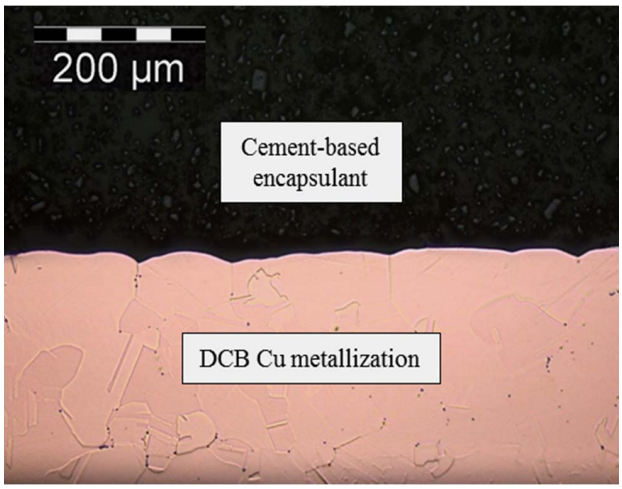

Figure 13. Contact interface of the cement-based encapsulant to the copper metallization of the DCB substrate.

C. *Power cycling and failure analysis*

1) Power cycling results: First power cycling tests were conducted to compare the reliability behavior of MiniPIM modules with silicone gel and cement-based encapsulation close to real application conditions. Within this preliminary study, a PC-based encapsulation was selected for testing. Figure 14 shows the Weibull plots of the power cycles until end of life (EOL) in comparison of silicone gel- (red lines) and PC-based encapsulation (blue lines). The dotted lines represent a confidence range of 95 %. The result indicates a striking difference in lifetime by a factor of 3.5 since the modules with a standard silicone gel encapsulation failed at a characteristic Weibull value of about 20.000 cycles compared to about 70.000 cycles for the PC-encapsulated samples.

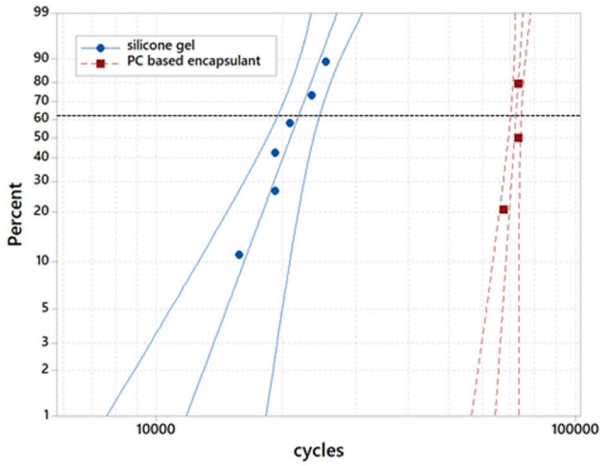

Figure 14. Weibull plot of the failure probability as a function of the number of power cycles till EOL of modules with standard silicone gel encapsulation (blue lines) in comparison to modules with PC-based encapsulation. The bold lines are Weibull fits and the thin lines indicate the related 95 % confidence intervals.

2) Failure analysis: Subsequent to power cycling the modules were inspected by non-destructive CT X-ray analysis. Afterwards they were opened for optical and SEM analysis using Ardrox 2312 [26] for the decapsulation of the silicone gel and a special cement solvent [27] for the decapsulation of the cement-based encapsulants. In addition, cross-sections of the IGBT wire bonding contacts were prepared for a more detailed investigation of the particular failure modes. Figure 15 shows exemplarily the IGBT top-side of a power module with standard silicone gel encapsulation after power cycling. The module failed after approximately 20.000 cycles by bonding wire-lift-off, which is a typical failure mode under power cycling [16]. Bonding wires marked with blue arrows show a characteristic power cycling lift-off pattern. Contacts marked with red arrows showing thermal damages, probably due to the increased electrical stress on the remaining bonding wire contacts after the first fails.

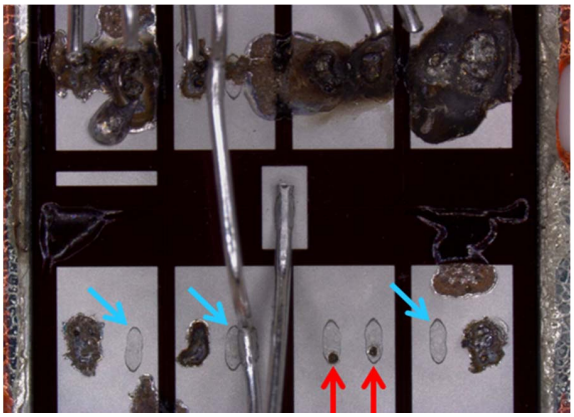

Figure 15. IGBT top-side after power cycling test of a power module with standard silicone gel encapsulation. Failure occuered after 20.000 cycles.

Figure 16 shows a higher resolution image of the footprint of a classic bond wire lift-off. Residues of bond wire material can still be detected on the surface of the chip metallization, indicating a crack formation and propagation within the aluminum material of the bonding wire.

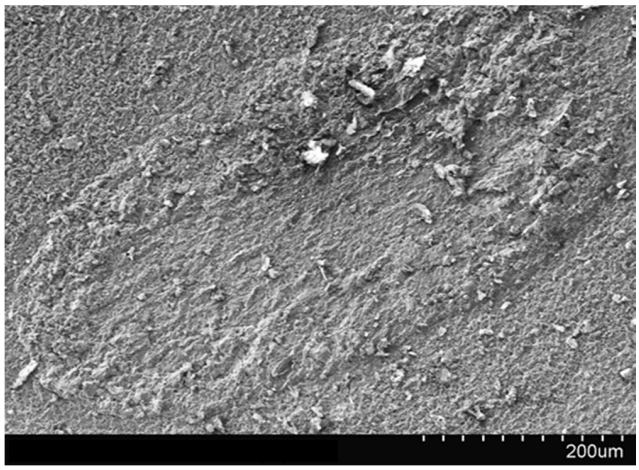

Figure 16. Lift-off pattern of a wire bond wedge after power cycling for a miniPIM module with standard silicone gel encapsulation.

Figure 17 supports this assumption by a cross sectional analysis of a remaining bond wire contact. The crack formation does not occur directly at the interface between bond wire and chip metallization, but it emerges partially in the volume of the bond wire.

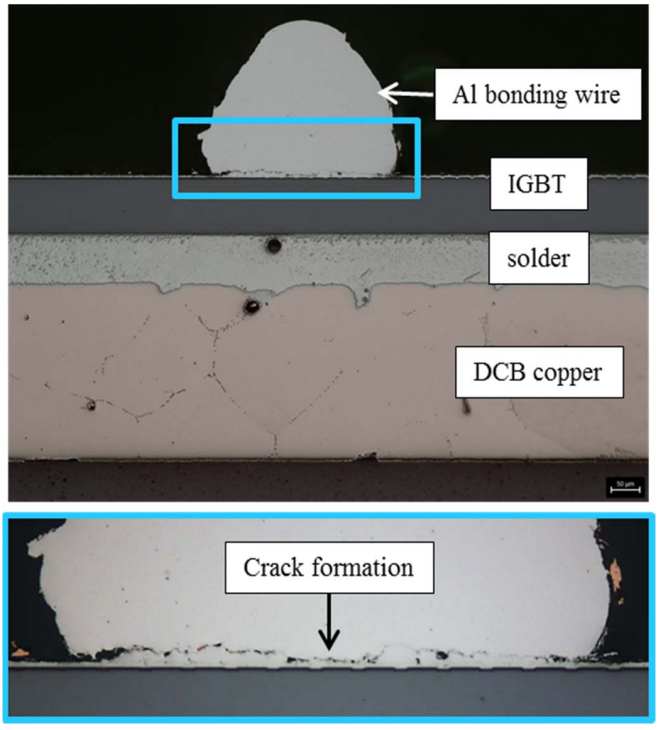

Figure 17. Cross section of a wire bond wedge with crack formation after power cycling (light microscopic images).

For comparison, Figure 18 shows the IGBT top-side contact of a tested MiniPIM module with PC-based encapsulation that reached its EOL after approximately 70.000 cycles.

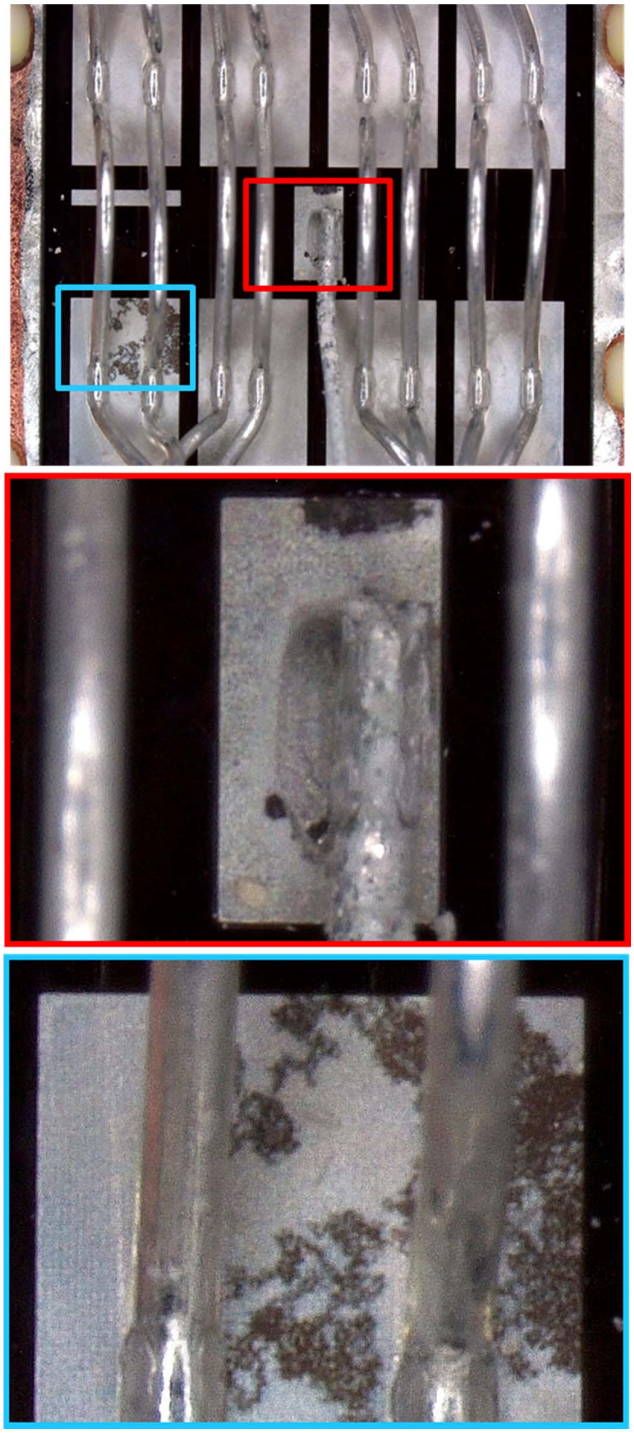

Figure 18. Tested IGBT of the cement encapsulated module with beginning aluminum surface reaction.

In contrast to the module with silicone gel encapsulation, no wire lift offs have been detected. However, for the bonding wire contacts marked by the red and the blue rectangle in the upper part of Figure 18 indication of interaction effects at both the Al bond wire surface and the Al chip metallization was detected, visualized by the central and lower parts in Figure 18. Similar effects were also observed at test vehicles after H^3TRB testing. These preliminary results indicate that the failure mode of the PC-based encapsulated modules shifts from a wire bond lift-off to a chip metal modification caused by reactive cement components or additives. It can be hypothesized that lift-offs are prevented by the lower thermal expansion and the higher stiffness of the cement-based encapsulation, reducing the thermomechanical displacement of the Al wire. On the other hand, these results do again underline the need for further improvements aiming at a material compatibility of the cements with the electronic components, which is in the current focus of further material development. However, the lifetime increase of factor 3.5 shows the enormous potential of the new cement-based materials.

In addition to the analysis of the top-side contacts, also the situation at the die attach was analyzed. Figure 19 compares the chip-solder interface of a module with standard silicone gel encapsulation (Figure 19 a)) and a module with PC-based encapsulation (Figure 19 b)).

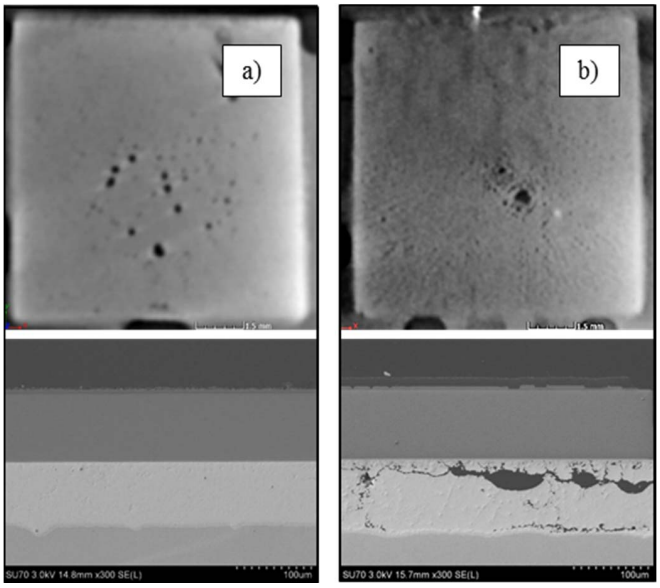

Figure 19. X-Ray immages (top) and SEM cross section analysis (bottom) of the chip solder of IGBT power modules after power cycling: a) Standard silicone gel encapsulation (20.000 cycles till EOL): no solder degradation, b) cement-based encapsulation (70.000 cycles till EOL): solder degradation due to the high number of power cycles.

Images on top of Figure 19 represent results of X-ray analysis, while images on the bottom show the results from SEM cross section analysis. A more distinct degradation in the solder contact of the cement-based encapsulated module becomes obvious. This is easily explained by the much

higher number of cycles to failure for the modules with PC-based encapsulation. On the other hand, it indicates another failure mode in addition to Al modification that has to be considered during future investigations.

V. SUMMARY AND OUTLOOK

The paper introduces novel PC- and CAC-based material systems with enhanced thermal, mechanical and thermomechanical properties for the encapsulation of power electronic devices and modules. These materials are aiming at improving the high-temperature operation potential of power electronic systems and thus, to promote a successful application of wide bandgap power devices in power electronics.

Within the current study, special attention was given to a thorough material characterization of the new encapsulants including high resolution microstructural analysis and the characterization of the thermomechanical behavior based on mechanical testing and micromechanical material modeling, the investigation of interactions at electronic material interfaces and on the reliability behavior of cement encapsulated power devices under active power cycling. The main results are:

- The microstructural composition of the cement-based encapsulants, such as filler content, -size and -distribution has an enormous impact on the resulting material properties like the CTE, thermal conductivity and Young's modulus. This allows a specific adaption of the material properties of cement-based encapsulants for particular applications.
- The combination of microstructural characterization methods and material modeling provides a more rapid screening of the influence of different filler particles and other structural features, such as pores or voids, on the resulting thermal, mechanical and thermomechanical characteristics as a function of the cement composition. Thus, the approach aims at supporting and accelerating the material development and microstructure design optimization by reducing the time of development and the experimental efforts.
- The results from microstructural modelling gives also guidelines and recommendations for further material improvements. Furthermore, it provides important input parameters and variables for future finite element (FEA) simulations in order to predict the reliability and lifetime characteristics of cement-encapsulated systems.
- The analysis of interface reactions was used to identify and to exclude potential defect risks at an early stage of development. A novel failure mechanism observed in this study is the reaction of Al bonding wires and the Al top-side metallization of power semiconductors with the cement-based encapsulants after extensive thermomechanical and electrical stressing the respective test vehicles.
- The results of power cycling tests indicate a striking difference in lifetime by a factor of 3.5 between standard silicone gel encapsulated and PC-encapsulated power modules, meaning an immense reliability improvement of power modules with cement-based encapsulation.
- Preliminary results from a subsequent failure analysis indicate that the failure mode of the PC-based encapsulated modules shifts from a wire bond lift-off (failure mode of standard silicone gel modules) to a chip metal degradation.

The results underline the enormous potential of the new cement-based encapsulants but also reveal need for further development. Thus, future basic and application-oriented investigations will be conducted to tap the full potential of CAC and PC-based encapsulants in power electronics packaging. This includes:

- Further material development supported by microstructural characterization and material design to achieve best possible thermal, mechanical and thermomechanical behavior and to generate input parameters and variables for future finite element (FEA) simulations in order to predict the reliability and lifetime characteristics of highly integrated, power electronic Si, GaN or SiC modules based on the new encapsulation materials.
- Optimization of the cement formulation to enhance the compatibility with electronic materials at contact interfaces, especially for Al bonding wires and Al top-side metallizations, to avoid degradation effects and to further increase reliability and lifetime of cement-encapsulated power modules.
- Further reliability testing including power cycling, HTRB, H^3TRB and thermal cycling in combination with comprehensive failure analysis to fully explain the life-time limiting effects of cement-encapsulated modules.
- A deeper investigation of the positive lifetime enhancing effects of cement-based encapsulants in power cycling tests, supported by static and dynamic thermomechanical simulation. These numerical studies will also help to understand the impact of the higher thermal conductivity of cement-based encapsulants on the reliability.

Finally, on example of novel cement-based encapsulants, the paper underlines the importance of material enhancement and development in power electronics packaging to achieve improved reliability with high-temperature operation. The study further demonstrates how microstructural investigations and a detailed failure analysis helps to identify and to exclude potential defect risks at an early development stage, thus providing guidance for technology optimization with regard to high quality and reliability during future application.

ACKNOWLEDGMENT

The work presented received financial support by the Federal Ministry of Education and Research BMBF (Contract: 16EMO0226).

REFERENCES

[1] R. W. Johnson, J. L. Evans, P. Jacobsen, J. R. Thompson and M. Christopher, "The changing automotive environment: high-temperature electronics," in IEEE Transactions on Electronics Packaging Manufacturing, vol. 27, no. 3, pp. 164-176, July 2004, doi: 10.1109/TEPM.2004.843109.

[2] P. J. Wellmann, "Power Electronic Semiconductor Materials for Automotive and Energy Saving Applications - SiC, GaN, Ga_2O_3, and Diamond," Zeitschrift Für Anorganische Und Allgemeine Chemie, 643(21), 1312-1322, 2017, doi:10.1002/zaac.201700270.

[3] L. Bartolomeo et al., "Wide Band Gap Materials: Revolution in Automotive Power Electronics," Society of Automotive Engineers of Japan, Inc., 2016.

[4] P. Dietrich, "Trends in automotive power semiconductor packaging," Microelectronics Reliability, vol. 53, Issues 9-11, pp. 1681-1686, September-November 2013, doi: 10.1016/j.microrel.2013.07.088.

[5] A. Mavinkurve, L. Goumans and J. Martens, "Epoxy molding compounds for high temperature applications," 2013 Eurpoean Microelectronics Packaging Conference (EMPC), Grenoble, 2013, pp. 1-7.

[6] J. Falbe, M. Regitz, B. Fugmann, S. Lang-Fugmann, W. Steglich, „Römpp-Lexikon," Naturstoffe, Georg Thieme, Stuttgart,1997.

[7] A. D. Wilson and J. W. Nicholson, "Acid-base cements: their biomedical and industrial applications," Cambridge University Press, Cambridge 1993.

[8] A. S. Wagh, "Recent Progress in Chemically Bonded Phosphate Ceramics," ISRN Ceramics, vol. 2013, Article ID 983731, 20 pages, 2013. doi:10.1155/2013/983731.

[9] F. Götz-Neunhoeffer, "Modelle zur Kinetik der Hydratation von Calciumaluminatzement mit Calciumsulfat aus kristallchemischer und mineralogischer Sicht," Erlanger Forschungen / Reihe B, Naturwissenschaften und Medizin, 2006, 29:10.

[10] Y. Wang, X. Li, B. Zhu, P. Chen, "Microstructure evolution during the heating process and its effect on the elastic properties of CAC-bonded alumina castables," Ceramics International, 2016, 42:11355-11362.

[11] W. E. et al., "Castable refractory concretes," International Materials Reviews, 2001, 46:145-167.

[12] B. Han et al, "Hydration behavior of spinel containing high alumina cement from high titania blast furnace slag," Cement and Concrete Research, 2016, 79:257–264.

[13] S. Kaessner et al., "Novel cement-based encapsulation material for electronic packaging," submitted to Journal of Cement and Concrete Composites, 2018.

[14] H. Pöllmann, "Calcium aluminate cements - Raw materials, differences, hydration and properties", Reviews in Mineralogy and Geochemistry, vol.74, no. 1, 2012, doi: 10.2138/rmg.2012.74.1.

[15] M. Petzold et al.,"Analytics for Power Electronic Components - Methods to figure out root causes of failures," 10th International Conference on Integrated Power Systems (CIPS), Stuttgart, 2018.

[16] J. Lutz, „Halbleiter-Leistungsbauelemente - Physik, Eigenschaften, Zuverlässigkeit," Berlin Heidelberg, Springer Viehweg, 2012.

[17] IEC 60747-9:2007: "Semiconductor devices - Discrete devices - Part 9: Insulated-gate bipolar transistors (IGBTs)," International standard, VDE Verlag, 2007.

[18] IEC 60749-5:2017: "Semiconductor devices - Mechanical and climatic test methods - Part 5: Steady-state temperature humidity bias life test," International Standard, VDE Verlag, 2017.

[19] ZVEI LV324: "Qualification of power electronic modules for components of motor vehicles," Edition 2014-02.

[20] Digimat-FE, http://www.mscsoftware.com/product/digimat

[21] B. R. Rogers, S. R. Wilson, T. S. Cale, "Localized Coorosion of Aluminium-1.5 % Copper: Thin Films Exposed to Photoresist Developing Solutinos," Journal of Vacuum Science Technology A, 1991, 9:1616-1621.

[22] J. Fauty, S. Strouse, J. Yoder, C. Acuna, P. Evard, "Al-Cu Metal Bond Pad Corrosion During Wafer Saw," The International Journal of Microcurcuits and Electronic Packaging, 2001, 24:19-29.

[23] M. van Soestbergen, et al., "Theory of aluminum metallization corrosion in microelectronics," Electrochimica Acta, 2010, 55: 5459-5469.

[24] A. F. Hollemann, E. Wiberg and N. Wiberg, "Lehrbuch der Anorganischen Chemie," 102. Eddition, Walter de Gruyter, Berlin 2007.

[25] J. Rudzki, M. Becker, R. Eisele, M. Poech, F. Osterwald, "Power Modules with Increased Power Density and Reliability Using Cu Wire Bonds on Sintered Metal Buffer Layers," 9th International Conference on Integrated Power Systems (CIPS), Nuremberg, 2016.

[26] Material Safety Data Sheet , "ARDROX® 2312," Version 1, Chemetall GmbH, Print Date 11/20/2007.

[27] Sicherheitsdatenblatt gem. 91/155/EWG, "GP-04-DC Gipslöser SPEED-03_04," DC Dental Central GmbH, Stand: Oktober 2004.